IEEE Access
Multidisciplinary ⋮ Rapid Review ⋮ Open Access Journal

Received April 15, 2020, accepted April 27, 2020, date of publication May 4, 2020, date of current version May 18, 2020.

Digital Object Identifier 10.1109/ACCESS.2020.2992134

Expedited Feature-Based Quasi-Global Optimization of Multi-Band Antenna Input Characteristics With Jacobian Variability Tracking

SLAWOMIR KOZIEL[1,2], (Senior Member, IEEE), AND ANNA PIETRENKO-DABROWSKA[2], (Senior Member, IEEE)

[1]Engineering Optimization and Modeling Center, Reykjavik University, 101 Reykjavik, Iceland
[2]Faculty of Electronics, Telecommunications and Informatics, Gdansk University of Technology, 80-233 Gdansk, Poland

Corresponding author: Anna Pietrenko-Dabrowska (anna.dabrowska@pg.edu.pl)

This work was supported in part by the Icelandic Centre for Research (RANNIS) under Grant 206606051, and in part by the National Science Centre of Poland under Grant 2017/27/B/ST7/00563.

ABSTRACT Design of modern antennas relies—for reliability reasons—on full-wave electromagnetic simulation tools. In addition, increasingly stringent specifications pertaining to electrical and field performance, growing complexity of antenna topologies, along with the necessity for handling multiple objectives, make numerical optimization of antenna geometry parameters a highly recommended design procedure. Conventional algorithms, particularly global ones, entail often-unmanageable computational costs, so alternative approaches are needed. This work proposes a novel method for cost-efficient globalized design optimization of multi-band antennas incorporating the response feature technology into the trust-region framework. It allows for unequivocal allocation of the antenna resonances even for poor initial designs, where conventional local algorithms fail. Furthermore, the algorithm is accelerated by means of Jacobian variability tracking, which reduces the number of expensive finite-differentiation updates. Two real-world antenna design cases are used for demonstration purposes. The optimization cost is comparable to that of local routines while ensuring nearly global search capabilities.

INDEX TERMS Antenna design, input characteristics, EM-driven design, trust-region methods, response features.

I. INTRODUCTION

Rapid development of cutting-edge technologies (e.g., 5G [1], internet of things [2], or wearable devices [3], including those for tele-medicine purposes [4]), leads to increasingly exacting requirements imposed on contemporary antenna structures. Among these, demands for miniaturization [5], multi-functionality [6], or multi-band operation [7] can be listed. In consequence, the complexity of the antenna geometries grows steadily, along with the number of design variables required for their parameterization. Satisfying stringent specifications pertaining to electrical and field performance while maintaining small antenna footprints makes the design closure task a truly challenging endeavor. Because simpler models, such as equivalent networks, are either unavailable or unreliable, full-wave electromagnetic (EM) tools have become mandatory.

Unfortunately, EM-driven design optimization in multi-dimensional parameter spaces is inevitably associated with massive EM simulations generating considerable CPU costs. This is the case even for local methods (gradient [8] or pattern search algorithms [9]), let alone global algorithms, nowadays extensively utilizing population-based metaheuristics (genetic algorithms [10], differential evolution [11], or particle swarm optimizers [12]).

To lessen the computational overhead, various approaches have evolved in the recent years. In the context of gradient-based algorithms, adjoint sensitivities constitute an attractive way of accelerating the design process [13], [14]. Yet, for the time being, only a few high-frequency simulation

The associate editor coordinating the review of this manuscript and approving it for publication was Liang-Bi Chen.

packages (e.g., CST Microwave Studio 2018 [15]; ANSYS HFSS 2019 [16]) support this technology. Another approach includes surrogate-based optimization (SBO) techniques, widely applied in antenna design [17]. The SBO routines exploit fast replacement models (surrogates) that can be of one of the two types: data-driven and physics based. The numerous examples of the data-driven surrogates (also referred to as approximation models) comprise polynomial regression [18], artificial neural networks [19], radial basis functions [20], kriging [21], support vector regression [22], Gaussian Process regression [23], or multidimensional rational approximation [24].

The primary advantages of the approximation models are their versatility and low evaluation cost. The surrogate is set up with the sole usage of the sampled data acquired from the system of interest; virtually no physical insight is required. Unfortunately, a usable predictive power of the surrogate can only be secured if the design space is sampled with sufficient density, necessary to account for the system output variations within the model domain. For this reason, usually large training data sets are required to construct functional surrogates, rapidly increasing with the number of antenna parameters (so called curse of dimensionality [25]). In practice, construction of the surrogates in parameter spaces of high dimensions can be successfully conducted only if the system outputs are weakly nonlinear. This is not the case for, e.g., multi-band antennas of sharp, resonant-like responses. Even more importantly, in real-world engineering applications, for the model to be truly useful for design purposes, it has to cover wide ranges of parameters [26], [27]. Satisfying this demand is challenging as the characteristic features of the responses, such as frequency allocation of the resonances, change rapidly across the design space [28], [29].

Whereas, in the construction of the physics-based surrogates, a system-specific knowledge is exploited [30], usually in the form of a simplified physical description of the system at hand. SBO techniques involving physics-based surrogates encompass, among others, space mapping [31], response correction algorithms [32], feature-based optimization [33], or adaptive response scaling [34]. In the case of antennas, the main disadvantage of the physics-based surrogates is that—due to the lack of alternatives—they are primarily obtained through coarse-mesh EM analysis and are therefore quite expensive. As a result, computational efficiency may be more problematic to secure even for SBO processes.

Here, a novel framework for expedited EM-driven design closure of multi-band antennas is proposed. The key concept is an application of the two mechanisms: (i) cost-effective trust-region (TR) gradient search with tracking of Jacobian variation throughout the optimization run, along with (ii) the response feature technology [35]. In the former procedure, the response gradient changes are monitored. Upon discovering stable sensitivity patterns, CPU-intensive finite differentiation (FD)-based gradient updates are omitted for a specific number of iterations proportional to the magnitude of the gradient difference. The response feature technology globalizes the search process by exploiting the frequency and level coordinates of the selected characteristics points rather than the entire antenna responses. This has an effect of ''flattening'' the functional landscape handled by the optimization process. The proposed framework is demonstrated using the dual- and triple-band uniplanar antennas. The results confirm that positioning of the antenna resonances can be achieved in a numerically effective manner even starting from poor initial designs where conventional local optimizers are prone to failure. The major contributions of this paper include: (i) incorporation of the response feature technology into trust-region gradient-based optimization framework, (ii) development of reduced-cost trust-region algorithm based on Jacobian variability monitoring, (iii) comprehensively demonstrated quasi-global search capabilities for multi-band antennas, (iv) demonstrated computational efficiency of the proposed framework, which is comparable to that of local search procedures (thus, dramatically lower than for routinely used population-based metaheuristics).

II. QUASI-GLOBALIZED FEATURE-BASED ANTENNA OPTIMIZATION WITH JACOBIAN CHANGE TRACKING

This section describes the two major components of the proposed framework, i.e., the response feature technology and the accelerated trust-region gradient algorithm with Jacobian change monitoring. The combination of the two techniques allows for a cost-efficient and quasi-global optimization of multi-band antennas as demonstrated by the numerical studies of Section III.

A. FEATURE-BASED OPTIMIZATION OF MULTI-BAND ANTENNAS

Fulfilling stringent specifications imposed on electrical and field antenna characteristics requires careful tuning of its geometry parameters. This process is referred to as the design closure and its ultimate goal is to improve the performance of the device at hand according to the selected quality metric, typically being a scalar function of the parameters. In the case of multiple performance figures, the objectives may be aggregated or handled through explicit or implicit constraints [36] (genuine multi-objective design, as in [37], is not considered here). A design closure problem is formulated as

$$\boldsymbol{x}^* = \arg\min_{\boldsymbol{x}} U\left(\boldsymbol{R}(\boldsymbol{x})\right), \tag{1}$$

where $\boldsymbol{R}$ denotes the EM-simulated antenna response, with $\boldsymbol{x} \in R^n$ being a vector of geometry parameters. In antenna design, $\boldsymbol{R}(\boldsymbol{x})$ usually refers to antenna characteristics (e.g., reflection coefficient, gain, axial ratio, or radiation pattern) that are of interest in a given design context. For multi-band antennas considered in this paper, a typical design problem is a frequency allocation of the antenna resonances and/or maximization of the fractional bandwidth at the desired operating frequencies. Here, the former case is considered and the adopted scalar objective function U is

formulated as follows

$$U(\boldsymbol{R}(\boldsymbol{x})) = \max_{f \in F} |S_{11}(\boldsymbol{x}, f)|, \tag{2}$$

where $S_{11}(x, f)$ denotes the antenna reflection being a function of $\boldsymbol{x}$ and frequency f, whereas F stands for the frequency range of interest. Local optimization routines with the objective function U formulated as in (2), may or may not succeed in finding the optimal solution depending on the quality of the initial design. In particular, due to high nonlinearity of antenna responses, especially for multi-band structures, the allocation of resonances at the initial design is critical for the success of the local search. Some typical scenarios have been illustrated in Fig. 1.

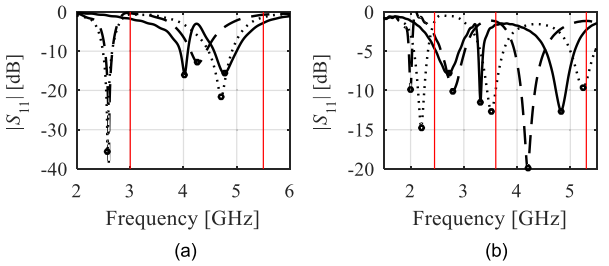

FIGURE 1. Exemplary reflection characteristics of (a) dual- [39]) and (b) triple-band antenna [40] at three different designs; characteristic points corresponding to the coordinates of the antenna resonances marked with (o); intended operating frequencies marked with vertical lines. Local (gradient-based) optimization routines starting from the designs (- - -) and (—) fail in the case of minimax formulation of the objective function as in (2). Local optimization involving response features finds satisfactory design starting from all the presented designs: (- - -), (—) and (...).

Employing global optimization routines to solve the antenna design closure task is associated with a high computational cost that can be conveniently reduced with the response feature approach [35]. Let us consider, for the illustration purposes and without losing generality, the feature points corresponding to the antenna resonances, i.e., $\boldsymbol{R}_F(\boldsymbol{x}) = [f_1(\boldsymbol{x}) f_2(\boldsymbol{x}) \ldots f_p(\boldsymbol{x}) \; l_1(\boldsymbol{x}) \; l_2(\boldsymbol{x}) \ldots l_p(\boldsymbol{x})]^T$, where f_k and l_k refer to the frequency and level coordinates of the respective p antenna resonances. The dependence of the feature point coordinates on the design variables is notably less nonlinear than for the responses themselves [35].

This is the reason for which, in most cases, a local search brings satisfactory designs even starting from poor initial ones, where the routines solving the problem (1) and (2) may fail. It should be emphasized that for the response-feature approach to work, it is sufficient that the initial design exhibits all the necessary features (i.e., clearly distinguished resonances in the case of a multi-band antenna), regardless of their specific frequency allocation or the levels.

The antenna design problem may be reformulated for the objective function $U_F(\boldsymbol{R}_F(\boldsymbol{x}))$ defined in terms of the response features $\boldsymbol{R}_F(\boldsymbol{x})$ in the following manner

$$\boldsymbol{x}^* = \arg\min_{\boldsymbol{x}} U_F\left(\boldsymbol{R}_F(\boldsymbol{x})\right). \tag{3}$$

In the case of relocating the resonances to the target frequencies of choice $f_{0.k}$, $k = 1, \ldots, p$, the objective function U_F is defined as

$$U_F(\boldsymbol{R}_F(\boldsymbol{x})) = \max\{l_1(\boldsymbol{x}), \ldots, l_p(\boldsymbol{x})\} + \\ +\beta ||[f_1(\boldsymbol{x}) \ldots f_p(\boldsymbol{x})] - [f_{0.1} \ldots f_{0.p}]||^2, \tag{4}$$

with β being the scalar penalty factor. In this paper, the antenna reflection is considered as the system output of interest and the level coordinates are $l_k(\boldsymbol{x}) = S_{11}(\boldsymbol{x}, f_k)$, $k = 1, \ldots, p$. In (4), minimization of the antenna reflection is the primary objective, whereas the second (penalty) term permits the control of the resonant frequencies of the antenna. The penalty factor β controls the 'hardness' of the constraint, i.e., it allows us to balance the contribution of the penalty term (measuring the discrepancies between the target and the actual operating frequencies of the antenna) and the primary objective. In the numerical experiments of Section III, we use $\beta = 100$ (note that frequencies are in GHz). This means that noticeable contribution from the penalty term can be observed for frequency deviations larger than 0.05 GHz or so. It should also be noted that the particular value of the penalty factor is not critical and the values from the range 10 to 500 could be used as well. If the bandwidth maximization is of interest, the design task can be formulated similarly, however, the response features corresponding to -10 dB levels of the reflection characteristic have to be used.

B. TRUST-REGION SEARCH EXPLOITING JACOBIAN CHANGES TRACKING

Here, the optimization procedure of choice to solve the problem (3) is the trust-region gradient search algorithm (e.g., [38]) that iteratively yields approximations $\boldsymbol{x}^{(i)}$, $i = 0, 1, \ldots$, to the optimum design $\boldsymbol{x}^*$. The flow diagram of the TR procedure is shown in Fig. 2. In each i-th iteration, a linear expansion model $\boldsymbol{R}_{lin}^{(i)}$ of $\boldsymbol{R}_F(\boldsymbol{x})$ is defined $\boldsymbol{x}^{(i)}$ as

$$\boldsymbol{R}_{lin}^{(i)}(\boldsymbol{x}, f) = \boldsymbol{R}_F(\boldsymbol{x}^{(i)}) + \boldsymbol{J}_F(\boldsymbol{x}^{(i)}) \cdot (\boldsymbol{x} - \boldsymbol{x}^{(i)}). \tag{5}$$

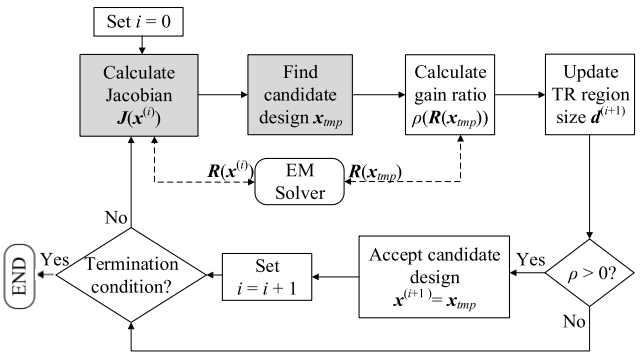

FIGURE 2. Flow diagram of the trust region (TR) algorithm. The grey boxes refer to the operations that are dissimilar for the conventional and feature-based versions of the algorithm; both with and without Jacobian change tracking.

Subsequently, the following sub-problem is solved

$$\boldsymbol{x}^{(i+1)} = \arg\min_{\boldsymbol{x};\; -\boldsymbol{d}^{(i)} \le \boldsymbol{x} - \boldsymbol{x}^{(i)} \le \boldsymbol{d}^{(i)}} U_F(\boldsymbol{R}_{lin}^{(i)}(\boldsymbol{x})). \tag{6}$$

In (5), $\boldsymbol{J}_F(\boldsymbol{x}^{(i)}) = [\nabla f_1(\boldsymbol{x}^{(i)}) \ldots \nabla f_p(\boldsymbol{x}^{(i)}) \nabla l_1(\boldsymbol{x}^{(i)}) \ldots \nabla l_p(\boldsymbol{x}^{(i)})]^T$ refers to the response feature vector Jacobian.

In addition, $\boldsymbol{d}^{(i)}$ stands for the search region size vector adjusted in conformance with the standard rules (e.g., [38], based on the gain ratio $\rho = (U_F(\boldsymbol{R}_F(\boldsymbol{x}_{tmp})) - U_F(\boldsymbol{R}_F(\boldsymbol{x}^{(i)})))/(U_F(\boldsymbol{R}_{lin}^{(i)}(\boldsymbol{x}_{tmp})) - U_F(\boldsymbol{R}_{lin}^{(i)}(\boldsymbol{x}^{(i)})))$, where $\boldsymbol{x}_{tmp}$ is the candidate design obtained in the $(i+1)$th iteration. The inequalities $-\boldsymbol{d}^{(i)} \le \boldsymbol{x} - \boldsymbol{x}^{(i)} \le \boldsymbol{d}^{(i)}$ in (6) are to be interpreted component-wise. This is to ensure similar handling of the variables with significantly different ranges, commonly occurring in the antenna design.

Unless adjoint sensitivities [13] are readily available, the Jacobian $\boldsymbol{J}_{\boldsymbol{R}}$ has to be estimated through finite differentiation (FD) at the expense of n additional antenna EM model simulations. In this paper, in order to lessen this cost, an expedited procedure is utilized where some of the FD-based Jacobian updates are omitted for the variables that exhibit stable sensitivity pattern. The variations of the Jacobian $\boldsymbol{J}_F$ columns $J_k^{(i)} = [g_{.1}^{(i)} \ldots g_{.n}^{(i)}]^T$, $k = 1, \ldots, p$, between iterations are assessed by the following metric:

$$\Delta_k^{(i+1)} = \frac{1}{2p} \sum_{j=1}^{2p} \left(2 \cdot \frac{g_{j.k}^{(i)} - g_{j.k}^{(i-1)}}{g_{j.k}^{(i)} + g_{j.k}^{(i-1)}} \right). \tag{7}$$

In (7), averaging is performed over both the frequency and level coordinates of all relevant feature points. Let us define the following quantities:

- $\Delta^{(i)} = [\Delta_1^{(i)} \ldots \Delta_n^{(i)}]^T$ – a vector of Jacobian change factors at the i-th iteration;
- $\Delta_{\min}^{(i)} = \min\{\Delta_1^{(i)}, \ldots, \Delta_n^{(i)}\}$, $\Delta_{\max}^{(i)} = \max\{\Delta_1^{(i)}, \ldots, \Delta_n^{(i)}\}$;

$\boldsymbol{N}^{(i)} = [N_1^{(i)} \ldots N_n^{(i)}]^T$ – a vector of the numbers of upcoming iterations without FD, calculated in the i-th iteration with the use of the conversion function

$$N_k^{(i)} = \left[\left[N_{\max} + a^{(i)}(\Delta_k^{(i)} - \Delta_{\min}^{(i)}) \right]\right]. \tag{8}$$

with $N_{\min}$ and $N_{\max}$ being the algorithm control parameters that refer to the minimum and the maximum number of iterations without FD; and $a^{(i)} = (N_{\max} - N_{\min})/(\Delta_{\min}^{(i)} - \Delta_{\max}^{(i)})$; where the nearest integer function is denoted as $[[.]]$. The flow diagram of the gradient update procedure has been shown in Fig. 3.

In the proposed algorithm, the following rules apply:

1) Factors $\Delta_k^{(i)}$ are preserved throughout all iterations without FD and employed to establish $\Delta_{\min}^{(i)}$ and $\Delta_{\max}^{(i)}$ (i.e., they affect $N_k^{(i)}$ for other parameters);
2) $N_k^{(i)}$ is proportional to the magnitude of the gradient variation as assessed by the factors $\Delta_k^{(i)}$. For the variables featuring the smallest Jacobian changes between subsequent iterations ($\Delta_k^{(i)} = \Delta_{\min}^{(i)}$), the highest number of the suppressed updates is appointed i.e., $N_k^{(i)} = N_{\max}$. Furthermore, following the definition of the conversion function (8), the FD-based updates are performed at least once per $N_{\max}$ iterations;

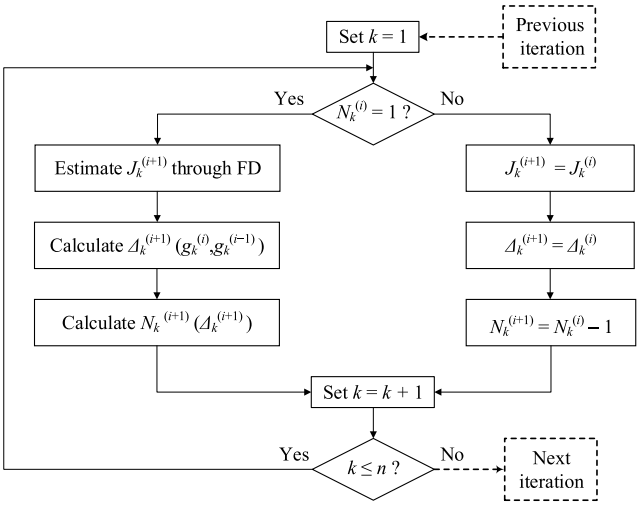

FIGURE 3. Flow diagram of the gradient update procedure utilized for both the conventional and feature-based optimization.

3) For the variables with the FD update, the components $N_k^{(i+1)}$ of the vector $\boldsymbol{N}^{(i+1)}$ are determined through the conversion function (8); otherwise the previous number of iterations is decremented, i.e., $N_k^{(i+1)} = N_k^{(i)} - 1$.

TABLE 1. Taxonomy of considered optimization procedures.

Algorithm	Problem formulation	Acceleration mechanism	Initial gradient estimation	Finite differentiation gradient update
1	Conventional	N/A	FD	Performed in each iteration for each parameter
2	Conventional	measure of changes of the response gradient between iterations	FD	Omitted in some iterations for some parameters
3	Feature-based	N/A	FD	Performed in each iteration for each parameter
4	Feature-based	measure of changes of the response gradient between iterations	FD	Omitted in some iterations for some parameters

In Table 1, a comparison of the main properties of the four algorithms considered in the paper is provided. Algorithms 1 and 2 are the conventional (with full FD Jacobian update) and the expedited TR routines, respectively, both solving a conventionally formulated problem (1). Algorithms 3 and 4 are, respectively, the conventional and the expedited versions solving the design task formulated in terms of the response features. Algorithms 1 through 3 are used for benchmarking purposes. The principal differences in operation of the fours algorithms include (see also Fig. 2):

1. Calculation of the Jacobian: either in terms of the entire response (Algorithms 1 and 2) or the response features (Algorithms 3 and 4);
2. Jacobian update procedure: either solely FD-based (Algorithms 1 and 3) or performed according to the

gradient change tracking procedure (Algorithms 2 and 4).

The proposed algorithm involving the gradient change control (this pertains to both Algorithm 2 and 4) operates as the reference algorithm merely in the first two iterations, when the Jacobian is estimated through FD. Full Jacobian data is required to determine the initial values of the factors $\Delta_k^{(i)}$. Subsequently, FD is only applied to the components J_k of $\boldsymbol{J}_F$ selected according to the sensitivity pattern measure; for other parameters, the former values of the factors $\Delta_k^{(i)}$ are retained (cf. Fig. 3). The numerical results gathered in Section III confirm that the proposed procedure secures considerable CPU cost savings. At the same time, a global search capability is maintained.

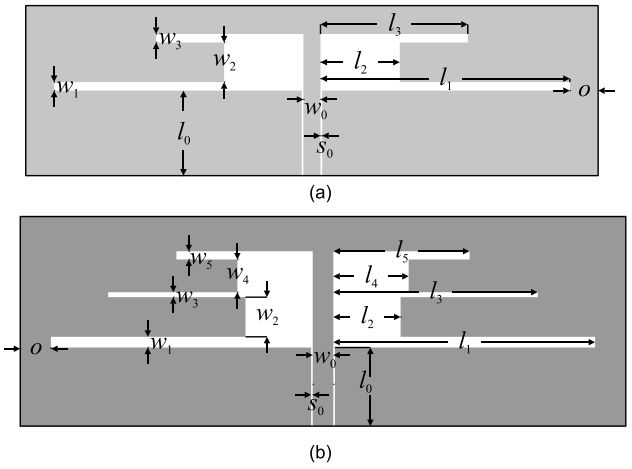

FIGURE 4. Benchmark uniplanar dipole antenna structures used for verification of the proposed algorithm: (a) dual- [39] and (b) triple-band [40] antenna.

III. VERIFICATION CASE STUDIES

This section provides a numerical verification of the proposed optimization framework and comparisons with conventionally formulated (not feature-based) procedures. The performance of the adopted approach is verified by analyzing the results obtained for multiple independent algorithm runs from random initial designs. Our benchmark set comprises two antenna structures: dual- [39] and triple-band [40] uniplanar dipoles shown in Fig. 4. Both structures are implemented on the RO4350 substrate ($\varepsilon_r = 3.48$, $h = 0.762$ mm) and fed by a coplanar waveguide. The geometry of the dual-band antenna (Antenna I) is described by the parameters $\boldsymbol{x} = [l_1\ l_2 l_3 w_1 w_2\ w_3]^T$, with the following variables fixed $l_0 = 30$, $w_0 = 3$, $s_0 = 0.18$ and $o = 5$ (all dimensions in mm). The antenna is supposed to operate at the center frequencies of 3 GHz and 5.5 GHz. The triple-band antenna (Antenna II) is described by the design variable vector $\boldsymbol{x} = [l_1 l_2 l_3 l_4\ l_5 w_1 w_2 w_3\ w_4 w_5]^T$; with $l_0 = 30$, $w_0 = 3$, $s_0 = 0.15$ and $o = 5$ being fixed (all dimensions in mm). The antenna is supposed to operate at the center frequencies of 2.45 GHz, 3.6 GHZ and 5.3 GHz. The EM antenna models are implemented in CST Microwave Studio and simulated

TABLE 2. Optimization results for antenna I.

Algorithm	Cost[a]	f_1[b] [GHz]	std(f_1)[c]	f_2[d] [GHz]	std(f_2)[e]	$\lvert S_{11}(f_{0,1})\rvert$[h] [dB]	$\lvert S_{11}(f_{0,2})\rvert$[i] [dB]
1	78.3	2.68	1.1	5.10	1.5	–8.4	–10.3
2	53.5	2.69	1.1	4.80	1.6	–9.6	–13.2
3	78.0	3.00	0.0	5.50	0.0	–38.8	–40.3
4	49.9	3.04	0.1	5.48	0.1	–27.1	–27.8

[a] Computational cost (average number of EM simulations; 20 algorithm runs).
[b,d,e] Resonance frequencies f_1, f_2 and f_3 averaged over the set of 20 algorithm runs.
[c,e,g] Standard deviations of resonance frequencies across the set of 20 algorithm runs.
[h,i,j] Antenna reflections for the required resonance frequencies in dB averaged over 20 algorithm runs.

TABLE 3. Optimization results for antenna II.

Algorithm	Cost[a]	f_1[b] [GHz]	std(f_1)[c]	f_2[d] [GHz]	std(f_2)[e]	f_3[f] [GHz]	std(f_3)[g]	$\lvert S_{11}(f_{0,1})\rvert$[h] [dB]	$\lvert S_{11}(f_{0,2})\rvert$[i] [dB]	$\lvert S_{11}(f_{0,3})\rvert$[j] [dB]	Cost[a]
1	50.5	2.19	0.8	2.98	1.1	4.70	1.7	–4.7	–4.3	–7.5	50.5
2	25.7	2.23	0.8	3.06	1.2	4.58	1.6	–4.9	–3.9	–4.6	25.7
3	83.9	2.45	0.0	3.60	0.0	5.31	0.0	–30.5	–31.4	–29.0	83.9
4	46.5	2.45	0.0	3.60	0.0	5.30	0.0	–27.1	–28.4	–25.6	46.5

[a] Computational cost (average number of EM simulations; 20 algorithm runs).
[b,d,e] Resonance frequencies f_1, f_2 and f_3 averaged over the set of 20 algorithm runs.
[c,e,g] Standard deviations of resonance frequencies across the set of 20 algorithm runs.
[h,i,j] Antenna reflections for the required resonance frequencies in dB averaged over 20 algorithm runs.

using its time-domain solver. Here, both antennas have been merely used for verification of the proposed framework, and no novel topology is introduced. The experimental validation of dual- and triple-band antenna structures can be found in [41]–[44].

Both antennas have been optimized using the algorithms of Table 1: conventional and expedited procedures solving a traditionally formulated problem (1) (Algorithms 1 and 2, respectively) and conventional and expedited procedures solving problem (3) reformulated in terms of response features (Algorithms 3 and 4, respectively). The expedited Algorithms 2 and 4 were executed with the following values of the control parameters: $N_{\min} = 1$, $N_{\max} = 5$. These parameters refer to the minimum and the maximum number of iterations without FD, respectively. They decide upon the frequency of performing FD-based sensitivity updates: not more than once per $N_{\min}$ iterations and at least once per $N_{\max}$ iterations. The adopted values allow us to achieve a substantial acceleration of the optimization process without compromising the solution quality in a significant manner.

In order to verify the robustness of the optimization process, each of the algorithms were executed twenty times from the same set of random initial designs. In Tables 2 and 3, the averaged performance measures for Antennas I and II across the set have been presented, and the antenna responses for the representative algorithm runs are shown in Figs. 5 and 6.

It should be emphasized that the values of the objective functions for the algorithms using conventional (Algorithms 1 and 2) and feature-based formulation

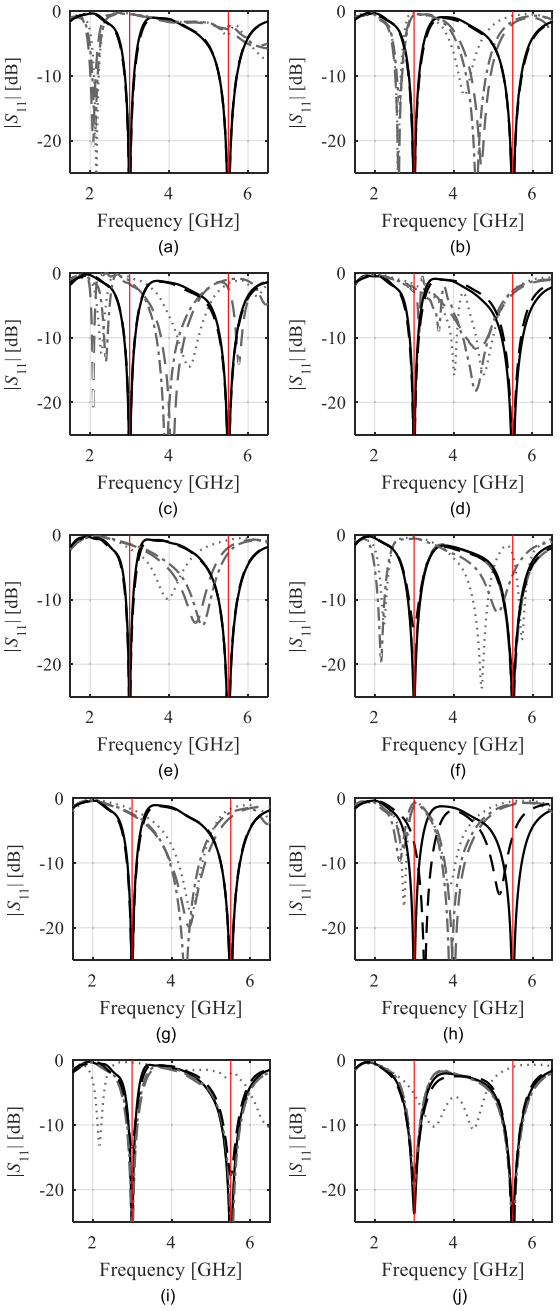

FIGURE 5. Operation of conventional routines for a dual-band antenna [39] (Algorithms 1 and 2), as well as their feature-based counterparts (Algorithms 3 and 4) for the representative algorithm runs starting from various initial designs: (1) reference TR algorithm with full FD Jacobian update, (2) expedited TR routine with Jacobian variability tracking, (3) basic version of the feature-based algorithm, and (4) expedited feature-based routine with Jacobian variability tracking. In each panel, the initial design (…) and the designs optimized with the use of conventional Algorithms 1 (- - -) and 2 (-.-.) are marked gray. Whereas the designs found within the response feature frameworks Algorithms 3 (—-) and 4 (- - -) are marked black. Vertical lines mark the target operating frequencies. The conventional routines (Algorithms 1 and 2) fail to find satisfactory designs in most cases.

(Algorithms 3 and 4) of the problem cannot be compared directly. Therefore, the comparison is carried out based on the feature point coordinates, which, for Algorithms 1 and 2, are extracted from the optimum responses obtained with these procedures.

As a measure of the results quality, Tables 2 and 3 report the standard deviation of the resonant frequencies obtained for the twenty algorithm runs executed. The computational cost in the form of total number of EM simulations required by the procedure to converge is also given in Tables 2 and 3.

The presented results (Tables 2 and 3, Figs. 5 and 6) allow us to draw certain conclusions concerning the algorithm performance. It can be observed that the feature-based algorithms (Algorithms 3 and 4) are superior over those solving a conventionally formulated design problem (Algorithms 1 and 2), both in terms of reliability and design quality.

For Antenna I, the reference conventional TR algorithm (Algorithm 1) fails to find satisfactory designs for a majority (14 out of 20) of the initial designs (cf. Fig. 5(a) through (h)). This is consistent with the results obtained for Antenna II, where Algorithm 1 fails to adequately allocate the antenna resonances for 18 out of 20 the considered starting points.

In the response features setup, however, Algorithm 3 accurately allocates the resonances for Antenna I and II in all cases (see Fig. 6). As far as the accelerated Algorithm 4 is concerned, for Antenna I, inadequate allocation of the resonant frequencies only occurs in four cases. For Antenna II, the designs satisfying the specifications are found in all cases.

Detailed scrutiny of the gathered results indicates that in the response feature framework, satisfactory designs can be found for a wide range of initial allocation of the antenna resonances. This is also the case for Antenna II, where for all the initial designs the feature-based algorithm yields excellent solutions.

In fact, as illustrated in Fig. 6, for Antenna II, the resonant frequencies of the initial design have to be close to the target ones (cf. Fig. 6(j)), for the conventional procedure to find an acceptable solution. The aforementioned variety of initial resonant frequency configurations as well as a comprehensive validation using a large number of random starting points demonstrates the quasi-global capabilities of both feature-based algorithms. The accelerated feature-based procedure (Algorithm 4) also exhibits a considerably improved computational efficiency.

The resonance depths in the conventional optimization setup for both antennas are poor. For Antenna I and Algorithm 1, the value −9 dB on average (for two resonances) is obtained; it is even worse for Antenna II (around −5.5 dB for three resonances). This is partially related to inadequate allocation of the resonant frequencies. It should be emphasized that the maximum acceptable level of antenna reflection at its operating frequencies is −10 dB. On the other hand, in the feature-based setup, the design quality is significantly better. For Antenna I, the reflection level is around −40 dB for the non-accelerated routine (Algorithm 3), and −27.5 dB on average for the accelerated one (Algorithm 4). Whereas for Antenna II, the obtained average values are −30 dB and −27 dB for Algorithms 3 and 4, respectively.

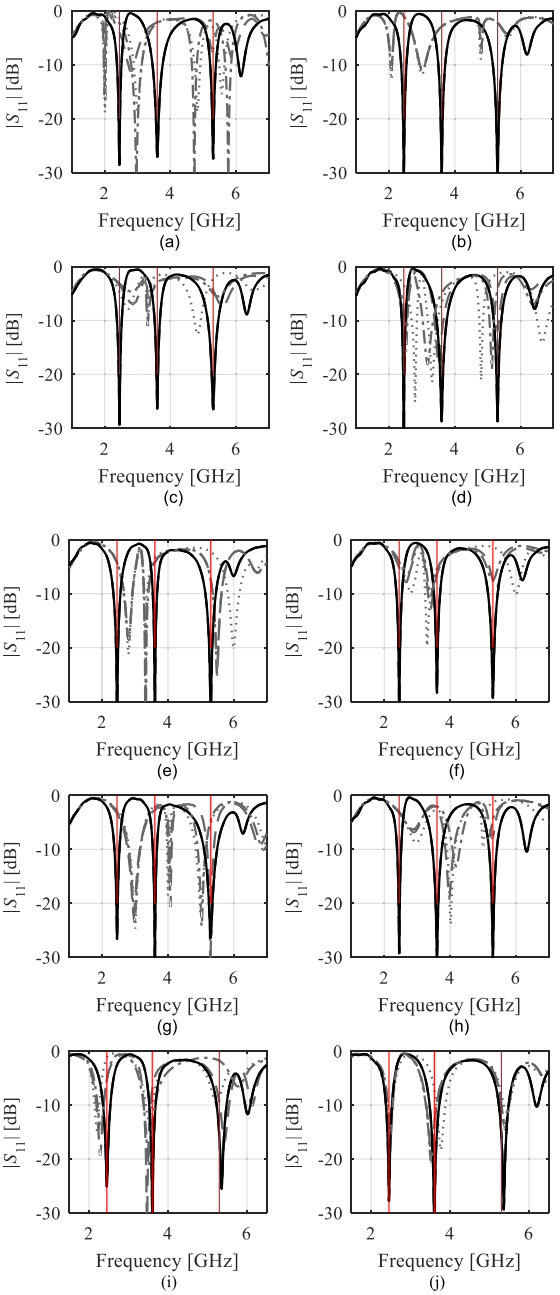

FIGURE 6. Operation of conventional routines for a triple-band antenna [40] (Algorithms 1 and 2), as well as their feature-based counterparts (Algorithms 3 and 4) for the representative algorithm runs starting from various initial designs: (1) reference TR algorithm with full FD Jacobian update, (2) expedited TR routine with Jacobian variability tracking, (3) basic version of the feature-based algorithm, and (4) expedited feature-based routine with Jacobian variability tracking. In each panel, the initial design (…) and the designs optimized with the use of conventional Algorithms 1 (- - -) and 2 (-.-.) are marked gray. Whereas the designs found within the response feature frameworks Algorithms 3 (—-) and 4 (- - -) are marked black. Vertical lines mark the target operating frequencies. The conventional routines (Algorithms 1 and 2) fail to find satisfactory designs in most cases. The conventional routines (Algorithms 1 and 2) fail to find satisfactory designs in most cases. Furthermore, the accelerated version of the feature-based optimization procedure finds satisfactory designs as effectively as its conventional, non-accelerated version.

The most important aspect of the optimization process for multi-band antennas is a proper allocation of the resonant frequencies. As indicated in Tables 2 and 3, the feature-based algorithms (Algorithms 3 and 4) are far superior over the conventional ones with this respect.

In particular, the frequencies obtained in the proposed approach are almost equal to the target frequencies (within the resolution important for practical purposes) for both considered antenna structures. This is not the case for the conventional frameworks.

In order to assess the computational speedup provided by the procedures involving smart Jacobian updates, one has to compare the conventional procedures with their accelerated counterparts, i.e., Algorithm 1 versus 2 (formulated in the entire response sense), as well as Algorithm 3 versus 4 (feature-based ones). For Antenna I, the savings of around 32 and 37 percent are obtained, respectively. As for Antenna II, the savings are even more pronounced: 49% (Algorithm 2 w.r.t. Algorithm 1), and 45% (Algorithm 4 w.r.t. Algorithm 1). At this point it should become clear that the computational cost of the proposed approach is dramatically lower than the cost of population-based metaheuristics, routinely used for global search purposes, e.g., [45]–[48]. The latter, given any imaginable setup (population size and the number of iterations) would well exceed 1,000 antenna evaluations, which is one of the reasons why these methods are most often applied to handle analytical representations (e.g., array factor models [49]–[51], etc.). It is also well known that metaheuristics require careful tuning of control parameters and exhibit poor solution repeatability. Therefore, these sort of methods were not included in the benchmark pool.

IV. CONCLUSION

The paper proposed a computationally efficient algorithm for quasi-global optimization of input characteristics of multi-band antennas. In the presented framework, the antenna design closure task is handled by employing the response feature technique in conjunction with the Jacobian change monitoring procedure. The reliability of the framework has been comprehensively validated using uniplanar dual- and triple-band dipole antennas. It has been demonstrated to be significantly more reliable than the conventional gradient-based algorithms. In particular, the proposed algorithm yields satisfactory designs for a wide range of initial designs, where the local routines fail. Another advantage of the approach is a high precision of allocating the resonant frequencies of the antenna. Apart from reliability, exploitation of the Jacobian variability tracking technique permits significant computational savings, which are as high as forty percent (on average) as compared to the standard (non-accelerated) algorithm. The optimization cost is therefore comparable to that of local search routines. At the same time, nearly global search capabilities are secured. In summary, the relevance of the incorporated algorithmic solutions in the proposed framework has been verified, along with suitability of the approach for solving real-world antenna design problems. In the future work, antenna optimization for other performance figures, including, among others,

bandwidth maximization and realized gain improvement will be considered.

ACKNOWLEDGMENT

The authors would like to thank Dassault Systemes, France, for making CST Microwave Studio available.

REFERENCES

[1] H. Huang, X. Li, and Y. Liu, "5G MIMO antenna based on vector synthetic mechanism," *IEEE Antennas Wireless Propag. Lett.*, vol. 17, no. 6, pp. 1052–1055, Jun. 2018.
[2] H. Liu, Y. Cheng, and M. Yan, "Electrically small loop antenna standing on compact ground in wireless sensor package," *IEEE Antennas Wireless Propag. Lett.*, vol. 15, pp. 76–79, 2016.
[3] A. Kavitha and J. N. Swaminathan, "Design of flexible textile antenna using FR4, jeans cotton and teflon substrates," *Microsyst. Technol.*, vol. 25, no. 4, pp. 1311–1320, Apr. 2019.
[4] R. Pei, J. Wang, M. Leach, Z. Wang, S. Lee, and E. G. Lim, "Wearable antenna design for bioinformation," in *Proc. IEEE Conf. Comput. Intell. Bioinf. Comput. Biol. (CIBCB)*, Chiang Mai, Thailand, Oct. 2016, pp. 1–4.
[5] A. A. Omar and Z. Shen, "A compact and wideband vertically polarized monopole antenna," *IEEE Trans. Antennas Propag.*, vol. 67, no. 1, pp. 626–631, Jan. 2019.
[6] J. Zhang, S. Yan, and G. A. E. Vandenbosch, "Metamaterial-inspired dual-band frequency-reconfigurable antenna with pattern diversity," *Electron. Lett.*, vol. 55, no. 10, pp. 573–574, May 2019.
[7] M. A. Antoniades, A. Dadgarpour, A. R. Razali, A. Abbosh, and T. A. Denidni, "Planar antennas for compact multiband transceivers using a microstrip feedline and multiple open-ended ground slots," *IET Microw., Antennas Propag.*, vol. 9, no. 5, pp. 486–494, Apr. 2015.
[8] J. Nocedal and S. J. Wright, *Numerical Optimization*. 2nd ed. New York, NY, USA: Springer, 2006.
[9] L. M. Rios and N. V. Sahinidis, "Derivative-free optimization: A review of algorithms and comparison of software implementations," *J. Global Optim.*, vol. 56, no. 3, pp. 1247–1293, Jul. 2013.
[10] J. S. Smith and M. E. Baginski, "Thin-wire antenna design using a novel branching scheme and genetic algorithm optimization," *IEEE Trans. Antennas Propag.*, vol. 67, no. 5, pp. 2934–2941, May 2019.
[11] M. Li, Y. Liu, and Y. J. Guo, "Shaped power pattern synthesis of a linear dipole array by element rotation and phase optimization using dynamic differential evolution," *IEEE Antennas Wireless Propag. Lett.*, vol. 17, no. 4, pp. 697–701, Apr. 2018.
[12] Z. Medina, A. Reyna, M. A. Panduro, and O. Elizarraras, "Dual-band performance evaluation of time-modulated circular geometry array with microstrip-fed slot antennas," *IEEE Access*, vol. 7, pp. 28625–28634, 2019.
[13] A. Khalatpour, R. K. Amineh, Q. S. Cheng, M. H. Bakr, N. K. Nikolova, and J. W. Bandler, "Accelerating space mapping optimization with adjoint sensitivities," *IEEE Microw. Wireless Compon. Lett.*, vol. 21, no. 6, pp. 280–282, Jun. 2011.
[14] S. Koziel, F. Mosler, S. Reitzinger, and P. Thoma, "Robust microwave design optimization using adjoint sensitivity and trust regions," *Int. J. RF Microw. Comput.-Aided Eng.*, vol. 22, no. 1, pp. 10–19, Jan. 2012.
[15] *CST Microwave Studio*, Comput. Simul. Technol. AG, Darmstadt, Germany, 2018.
[16] *HFSS Release 19.0*, ANSYS, Canonsburg, PA, USA, 2019.
[17] S. Koziel and S. Ogurtsov, *Antenna Design by Simulation-Driven Optimization*. New York, NY, USA: Springer, 2014.
[18] R. Jin, W. Chen, and T. W. Simpson, "Comparative studies of metamodelling techniques under multiple modelling criteria," *Struct. Multidisciplinary Optim.*, vol. 23, no. 1, pp. 1–13, Dec. 2001.
[19] A. Rawat, R. N. Yadav, and S. C. Shrivastava, "Neural network applications in smart antenna arrays: A review," *AEU-Int. J. Electron. Commun.*, vol. 66, no. 11, pp. 903–912, Nov. 2012.
[20] M. Li, A. Abubakar, and T. M. Habashy, "A three-dimensional model-based inversion algorithm using radial basis functions for microwave data," *IEEE Trans. Antennas Propag.*, vol. 60, no. 7, pp. 3361–3372, Jul. 2012.
[21] J. Gong, F. Gillon, J. T. Canh, and Y. Xu, "Proposal of a kriging output space mapping technique for electromagnetic design optimization," *IEEE Trans. Magn.*, vol. 53, no. 6, pp. 1–4, Jun. 2017.
[22] J. P. Jacobs, "Bayesian support vector regression with automatic relevance determination kernel for modeling of antenna input characteristics," *IEEE Trans. Antennas Propag.*, vol. 60, no. 4, pp. 2114–2118, Apr. 2012.
[23] J. P. Jacobs, "Efficient resonant frequency modeling for dual-band microstrip antennas by Gaussian process regression," *IEEE Antennas Wireless Propag. Lett.*, vol. 14, pp. 337–341, 2015.
[24] G. S. A. Shaker, M. H. Bakr, N. Sangary, and S. Safavi-Naeini, "Accelerated antenna design methodology exploiting parameterized cauchy models," *Prog. Electromagn. Res.*, vol. 18, pp. 279–309, 2009.
[25] X. Wu, X. Peng, W. Chen, and W. Zhang, "A developed surrogate-based optimization framework combining HDMR-based modeling technique and TLBO algorithm for high-dimensional engineering problems," *Struct. Multidisciplinary Optim.*, vol. 60, no. 2, pp. 663–680, Aug. 2019.
[26] F. Feng, C. Zhang, W. Na, J. Zhang, W. Zhang, and Q.-J. Zhang, "Adaptive feature zero assisted surrogate-based EM optimization for microwave filter design," *IEEE Microw. Wireless Compon. Lett.*, vol. 29, no. 1, pp. 2–4, Jan. 2019.
[27] M. B. Yelten, T. Zhu, S. Koziel, P. D. Franzon, and M. B. Steer, "Demystifying surrogate modeling for circuits and systems," *IEEE Circuits Syst. Mag.*, vol. 12, no. 1, pp. 45–63, 1st Quart., 2012.
[28] S. Koziel and A. Bekasiewicz, "Sequential approximate optimisation for statistical analysis and yield optimisation of circularly polarised antennas," *IET Microw., Antennas Propag.*, vol. 12, no. 13, pp. 2060–2064, Oct. 2018.
[29] U. Ullah and S. Koziel, "A broadband circularly polarized wide-slot antenna with a miniaturized footprint," *IEEE Antennas Wireless Propag. Lett.*, vol. 17, no. 12, pp. 2454–2458, Dec. 2018.
[30] T. K. Sarkar, H. Chen, M. Salazar-Palma, and M. Zhu, "Lessons learned using a physics-based macromodel for analysis of radio wave propagation in wireless transmission," *IEEE Trans. Antennas Propag.*, vol. 67, no. 4, pp. 2150–2157, Apr. 2019.
[31] J. C. Cervantes-González, J. E. Rayas-Sánchez, C. A. López, J. R. Camacho-Pérez, Z. Brito-Brito, and J. L. Chávez-Hurtado, "Space mapping optimization of handset antennas considering EM effects of mobile phone components and human body," *Int. J. RF Microw. Comput.-Aided Eng.*, vol. 26, no. 2, pp. 121–128, Feb. 2016.
[32] S. Koziel and L. Leifsson, *Simulation-Driven Design by Knowledge-Based Response Correction Techniques*. Cham, Switzerland: Springer, 2016.
[33] S. Koziel, "Fast simulation-driven antenna design using response-feature surrogates," *Int. J. RF Microw. Comput.-Aided Eng.*, vol. 25, no. 5, pp. 394–402, Jun. 2015.
[34] S. Koziel and S. D. Unnsteinsson, "Expedited design closure of antennas by means of trust-region-based adaptive response scaling," *IEEE Antennas Wireless Propag. Lett.*, vol. 17, no. 6, pp. 1099–1103, Jun. 2018.
[35] S. Koziel and A. Bekasiewicz, "Simulation-driven size-reduction-oriented design of multi-band antennas by means of response features," *IET Microw., Antennas Propag.*, vol. 12, no. 7, pp. 1093–1098, Jun. 2018.
[36] H. Wang, M. Olhofer, and Y. Jin, "A mini-review on preference modeling and articulation in multi-objective optimization: Current status and challenges," *Complex Intell. Syst.*, vol. 3, no. 4, pp. 233–245, Dec. 2017.
[37] S. Koziel and A. Bekasiewicz, *Multi-Objective Design of Antennas Using Surrogate Models*. Singapore: World Scientific, 2016.
[38] A. R. Conn, N. I. M. Gould, and P. L. Toint, *Trust Region Methods* (MPS-SIAM Series on Optimization), Philadelphia, PA, USA: Society Industrial Applied Mathematics, 2000.
[39] Y.-C. Chen, S.-Y. Chen, and P. Hsu, "Dual-band slot dipole antenna fed by a coplanar waveguide," in *Proc. IEEE Antennas Propag. Soc. Int. Symp.*, Albuquerque, NM, USA, Jul. 2006, pp. 3589–3592.
[40] S. Koziel and A. Bekasiewicz, "Fast redesign and geometry scaling of multiband antennas using inverse surrogate modeling techniques," *Int. J. Numer. Model., Electron. Netw., Devices Fields*, vol. 31, no. 3, p. e2287, May 2018.
[41] S. Koziel and A. Pietrenko-Dabrowska, "Reduced-cost design closure of antennas by means of gradient search with restricted sensitivity update," *Metrol. Meas. Syst.*, vol. 26, no. 4, pp. 595–605, 2019.
[42] S. Koziel and A. Pietrenko-Dabrowska, "Performance-based nested surrogate modeling of antenna input characteristics," *IEEE Trans. Antennas Propag.*, vol. 67, no. 5, pp. 2904–2912, May 2019.
[43] J. A. Tomasson, S. Koziel, and A. Pietrenko-Dabrowska, "Quasi-global optimization of antenna structures using principal components and affine subspace-spanned surrogates," *IEEE Access*, vol. 8, pp. 50078–50084, 2020.
[44] S. Kozieł and A. Bekasiewicz, "Rapid design optimization of multi-band antennas by means of response features," *Metrol. Meas. Syst.*, vol. 24, no. 2, pp. 337–346, Jun. 2017.

[45] E. BouDaher and A. Hoorfar, "Electromagnetic optimization using mixed-parameter and multiobjective covariance matrix adaptation evolution strategy," *IEEE Trans. Antennas Propag.*, vol. 63, no. 4, pp. 1712–1724, Apr. 2015.
[46] E. BouDaher and A. Hoorfar, "Fireworks algorithm: A new swarm intelligence technique for electromagnetic optimization," in *Proc. IEEE Int. Symp. Antennas Propag. (APSURSI)*, Fajardo, Puerto Rico, Jun. 2016, pp. 575–576.
[47] M. Kovaleva, D. Bulger, B. A. Zeb, and K. P. Esselle, "Cross-entropy method for electromagnetic optimization with constraints and mixed variables," *IEEE Trans. Antennas Propag.*, vol. 65, no. 10, pp. 5532–5540, Oct. 2017.
[48] A. Lalbakhsh, M. U. Afzal, and K. P. Esselle, "Multiobjective particle swarm optimization to design a time-delay equalizer metasurface for an electromagnetic band-gap resonator antenna," *IEEE Antennas Wireless Propag. Lett.*, vol. 16, pp. 912–915, Sep. 2017.
[49] S. K. Goudos and J. N. Sahalos, "Design of large thinned arrays using different biogeography-based optimization migration models," *Int. J. Ant. Propag.*, vol. 2016, pp. 1–11, Sep. 2016.
[50] S. Banerjee and D. Mandal, "Array pattern optimization for steerable circular isotropic antenna array using cat swarm optimization algorithm," *Wireless Pers. Commun.*, vol. 99, no. 3, pp. 1169–1194, Apr. 2018.
[51] C. Wang, Y. Wang, Z. Wang, M. Wang, S. Yuan, and W. Wang, "Structural–electrical coupling optimisation for radiating and scattering performances of active phased array antenna?" *Int. J. Electron.*, vol. 105, no. 4, pp. 586–597, Apr. 2018.

SLAWOMIR KOZIEL (Senior Member, IEEE) received the M.Sc. and Ph.D. degrees in electronic engineering from the Gdansk University of Technology, Poland, in 1995 and 2000, respectively, the M.Sc. degrees in theoretical physics and in mathematics, in 2000 and 2002, respectively, and the Ph.D. degree in mathematics from the University of Gdansk, Poland, in 2003. He is currently a Professor with the School of Science and Engineering, Reykjavik University, Iceland. His research interests include CAD and modeling of microwave and antenna structures, simulation-driven design, surrogate-based optimization, space mapping, circuit theory, analog signal processing, evolutionary computation, and numerical analysis.

ANNA PIETRENKO-DABROWSKA (Senior Member, IEEE) received the M.Sc. and Ph.D. degrees in electronic engineering from the Gdansk University of Technology, Poland, in 1998 and 2007, respectively. She is currently an Associate Professor with the Gdansk University of Technology. Her research interests include simulation-driven design, design optimization, control theory, modeling of microwave and antenna structures, and numerical analysis.